MUSCAT Comprehensive Design Review: Cryostat

Document number	MSCAT-SYST-01
Document version	1.0
Issue date	22nd June 2016

Written by	Simon Doyle	Cardiff University
	Edgar Castillo	
Approved by		

Cardiff University
Prifysgol Caerdydd

Instituto Nacional de Astrofísica, Óptica y Electrónica
INAOE

Table of Contents

1 Introduction, design concept and review process 1
2 Broad design overview 1
3 Vacuum Vessel and mounting frames 2
3.1 Main vacuum vessel 2
3.2 Pulse Tube Cooler Mounting 3
3.3 Mounting 4
3.4 Window 4
3.5 DC and RF feedthroughs 5
3.6 Manual heat switches 6
3.7 Arrangement of top plate 6
3.8 Low emissivity lining 6
3.9 Vacuum vessel checklist 6
4 First Cryogenic Stage 6
4.1 Mechanical support and thermal isolation 7
4.2 Thermal connections, thermal sinking and feedthroughs 8
4.3 Radiation shields and optical baffles 9
4.4 First stage checklist 10
5 Second cryogenic stage 10
5.1 Mechanical support and thermal isolation 10
5.2 Thermal connections, thermal sinking and feedthroughs 11
5.3 Sorption fridge location and heat sinking 11
5.4 Heat switch contact point 12
5.5 Radiation shields and optical baffling 12
5.6 Cold amplifier mounting 12
5.7 Second stage checklist 13
6 First sub-K stage 13
6.1 Mechanical support 13
6.2 First sub-K stage checklist 14
7 Second sub-K stage 15
7.1 Mechanical support and thermal isolation 15
7.2 Heat switch contact point 16
7.3 Radiation and magnetic shielding 16
7.4 Cable feedthroughs 17
7.5 Dilution unit mounting point. 17
7.6 Cold optics mounting 17
7.7 Second sub-K stage checklist 17
8 Focal plane stage 18
8.1 Mechanical support 18
8.2 Cable feedthroughs, thermal links and cooling 18
8.3 Focal plane checklist 18
9 Optical baffling and filter provision 18

9.1 Optical baffling 18
9.2 Filter provision 19
10 Magnetic shielding provision 20
11 Assembly 20
12 Apendix 20
12.1 Mass breakdown 20

1 Introduction, design concept and review process

The MUSCAT cryostat is intended to be a versatile cryogenic platform providing cooling and provision for optics for an F3 focal plane cooled to 100mK. The philosophy behind this design requirement is to create a cryogenic platform that in the first instance will house a 1.1mm focal plane but can be easily adapted to host alternative Kinetic Inductance Detector (KID) based technologies hence providing opportunity for long-term collaboration between the UK and Mexico in detector and focal plane technology development. To this end the cryostat is designed to:

- Provide a 100mK focal plane – cold enough for any envisaged ground based KID technology (photometric or on-chip spectrometer).
- Provide a focal plane that can fill the 4" field of view of the LMT.
- Provide space for fully baffled F3 optics capable of diffraction limited performance at:
  - 1mm – baseline
  - 0.85mm – goal
- Baffling to be sufficient for:
  - Baseline - horn coupled architectures
  - Goal open array architectures.
- Design to incorporate sufficient magnetic shielding with provision for additional shielding if required (levels of magnetic shielding is not well specified for KID arrays).
- Provide space for five RF readout channels with associated cold amplifiers, cables, cold attenuators and DC blocks.
- Design to fit in a designated space on the M3 platform that does not clash with the Toltec optics or a potential third port. Switching between MUSCAT, Toltec and port 3 should be as simple as possible.
- Provide a cryostat that is adaptable for test wiring beyond the requirements of MUSCAT (potential for additional DC or RF cabling at any temperature stage.

At the time of writing this document the cryostat design is at an advanced stage but not complete to the level of finalising drawings. Each section of this report outlines the considerations taken into account in designing each stage. The review is to confirm that the proposed design is fit for purpose and that all potential points of failure have been recognised and addressed. Each section concludes with a list of review questions that should be satisfied before final designs and drawings are completed and machining of parts commences.

2 Broad design overview

To assist the reviewing process, a broad overview of the system is outlined in this section. Here we show the space where MUSCAT is intended to fit, the position of Toltec, the potential position of a third optical port and cross-sections of the MUSCAT system in its entirety to illustrate constraints on space and the optical chain.

The position of MUSCAT on the M3 platform is shown in Figure 1. Switching between MUSCAT, Toltec and port 3 is achieved by folding away or removing the MUSCAT / Toltec select mirror or the MUSCAT / Port 3 select mirror.

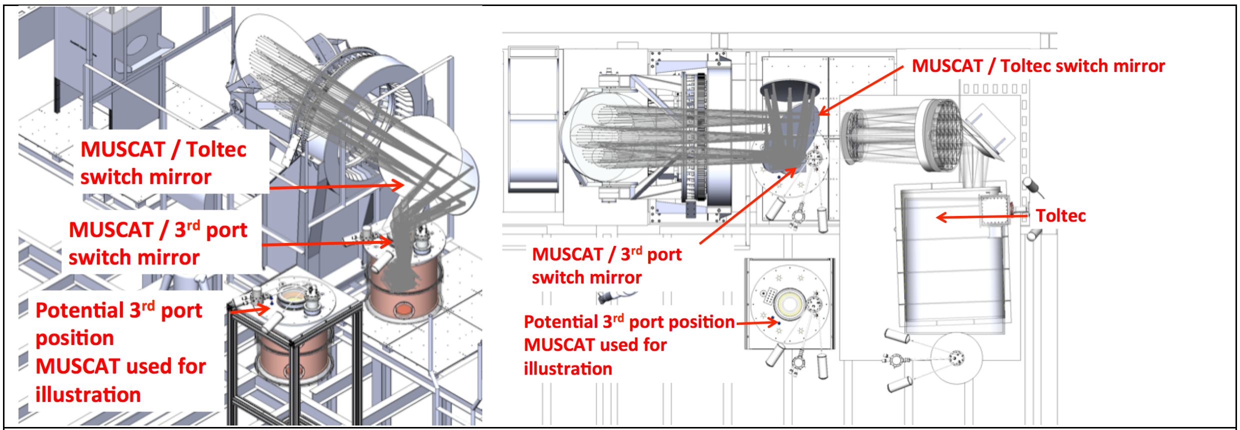

Figure 1 – MUSCAT located on the M3 platform.

Muscat will look upwards towards M4. It consists of the following clod stages:

- A first stage T ≈ 50K cooled by a pulse tube cooler
- A Second stage T ≈ 3.5K cooled by a pulse tube cooler
- A First sub-K stage T≈ 0.85 K cooled by continuous sorption cooler
- A Second sub-K stage T ≈ 0.35K cooled by continuous sorption cooler
- A focal plane stage T ≈ 0.1K cooled by continuous mini-dilution cooler

An overview of the cryostat is shown in Figure 2.

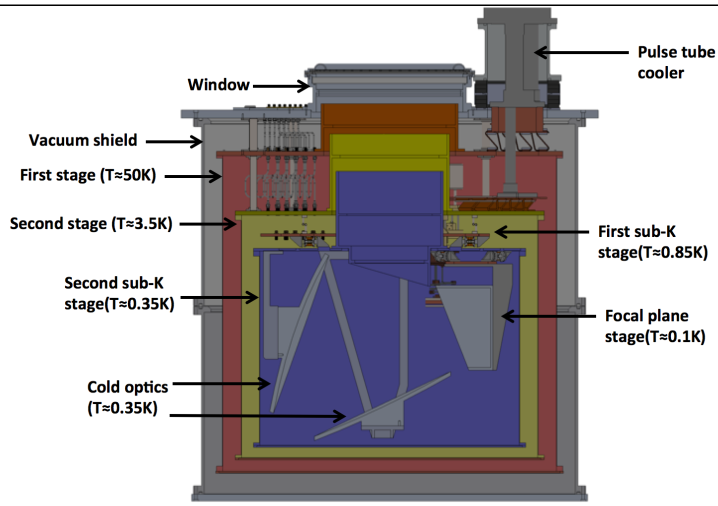

Figure 2 – MUSCAT overview

3 Vacuum Vessel and mounting frames

3.1 Main vacuum vessel

The vacuum vessel will reuse existing parts from a previous Cardiff experiment – CLOVER. While this approach somewhat limits the design freedom for MUSCAT, the cost savings enable a superior instrument to be developed within the limited budget. The existing Clover vacuum vessels have also been tested for structural integrity and vacuum performance hence reducing overall risk to the project. To accommodate the cryogenic components and cold optics of MUSCAT, two vacuum cans from CLOVER will be bolted together to achieve the required height.

MUSCAT will require a new vacuum base plate and top plate to accommodate the pulse tube cooler, window, DC and RF feedthroughs and mounting points. To reduce manufacture costs O-ring grooves will be cut into mating flanges that provide either wiring access points or blanking plates as outlined in Figure 3. These parts will be manufactured to the same thickness of Aluminium as used in the CLOVER system hence should not require further structural integrity analysis under a load of 1 atmosphere.

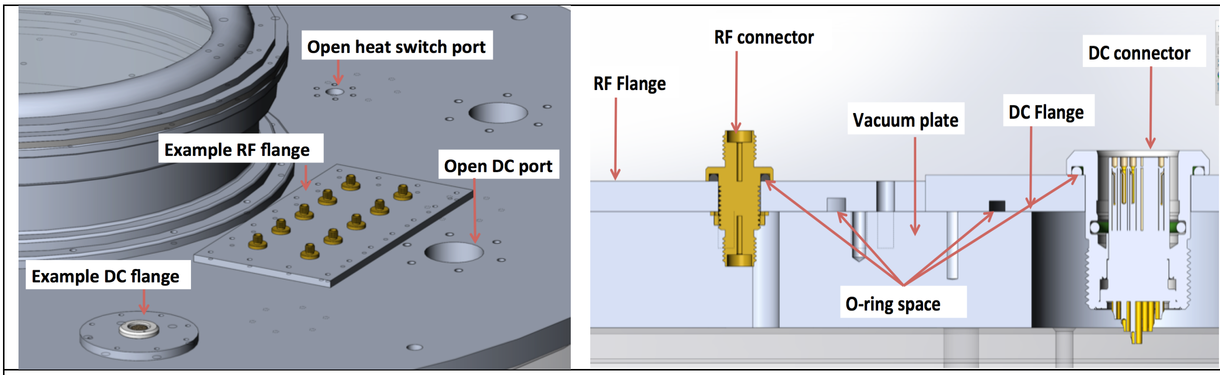

Figure 3: Cable feed-through points

3.2 Pulse Tube Cooler Mounting

The Pulse Tube Cooler (PTC) will be mounted to the top plate via a set of rubber damping gaskets. This method has been tried and tested with three systems build at Cardiff and provides sufficient vibrational damping from the PTC pulses as well as electrical isolation from the 3-Phase PTC power supply. Under vacuum the gaskets will compress. This effect is measured and taken into account in the design. The bolts holding the PTC in place are tightened under vacuum to keep the PTC assembly in a fixed position when the vessel is returned to atmospheric pressure. Connections of the PTC to cold stages in the cryostat is achieved via high thermal conductivity flexible cooper braid and therefore allows for around 20mm error in the PTC’s vertical position with respects to the rest of the cryostat assembly.

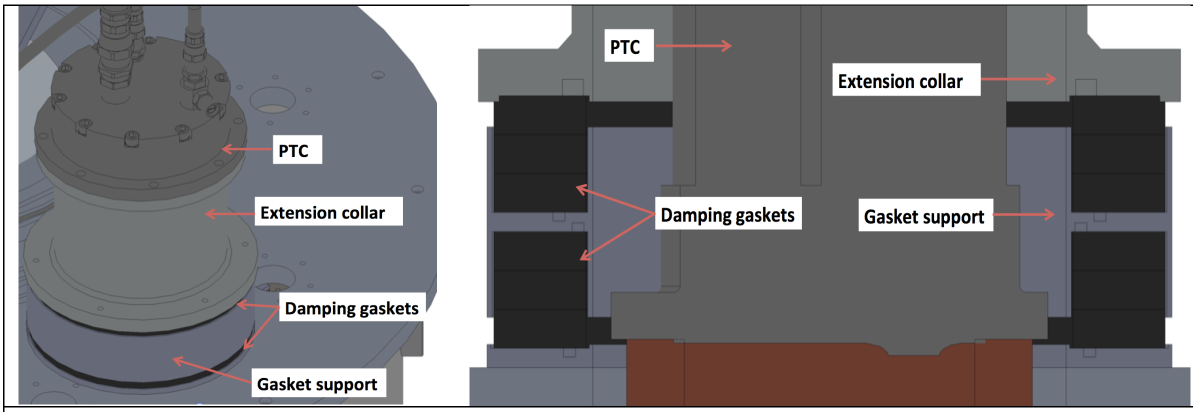

Figure 4: Vibrational damping Pulse Tube Cooler support

3.3 Mounting

The Vacuum vessel top plate also forms the mounting structure from which the entire system will hang and be adjusted in the vertical direction. The method for fixing and removing the vacuum cans and subsequent radiation shields is outlined later in this report. We envisage two frames to which MUSCAT will mount. A working frame for use in assembly and lab testing and a frame that will locate MUSCAT on the M3 platform and align with the warm optics at the LMT. We plan to design a transport mechanism that can be used to move MUSCAT between mounting frames at the LMT. The working mounting frame is shown in Figure 5.

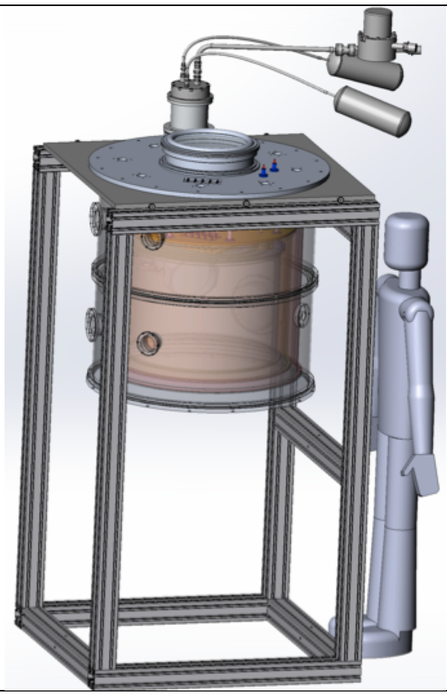

Figure 5: Mounting frame for working and assembly.

3.4 Window

We will use Ultra High Molecular Weight Polyethylene (UHWPE) as a window material. This material has been proven with instruments such as CLOVER and Actpol. CLOVER used a 15mm thick window with a diameter of 398mm that bows approximately 8mm at its centre under vacuum. The current MUSCAT design is slightly smaller with a diameter of 345mm so we will use the CLOVER design as our baseline. Actpol has proven these windows can be reduced in thickness to 6.86mm and still reliably hold vacuum. The technology exists at Cardiff to anti-reflection (AR) coat these windows for optimum in-band transmission. Figure 6 shows the example of the ACTpol window optimised for 150GHz. We will tune this window for envisaged MUSCAT bands. The ACTpol data shown in Figure 6 demonstrates that we can cover 180-330GHz with less than 5% loss in transmission due to fringing across the band.

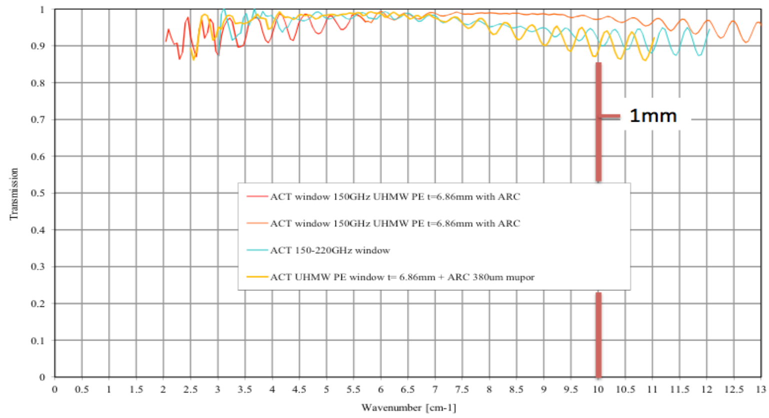

Figure 6: ACTPol window transmission

The window will be clamped to the cryostat via a rubber O-ring as used in clover. We will add a small dry air-gap space using a thin (negligible optical fringing and losses) Polypropylene sheet to prevent water condensation on the window. The space is kept dry by adding Silica Gel around the edges of the cavity. This is shown in Figure 7. Also shown in Figure 7 is a reflective baffle placed around the window edge designed to reduce the 300K radiation load on the 4K baffle.

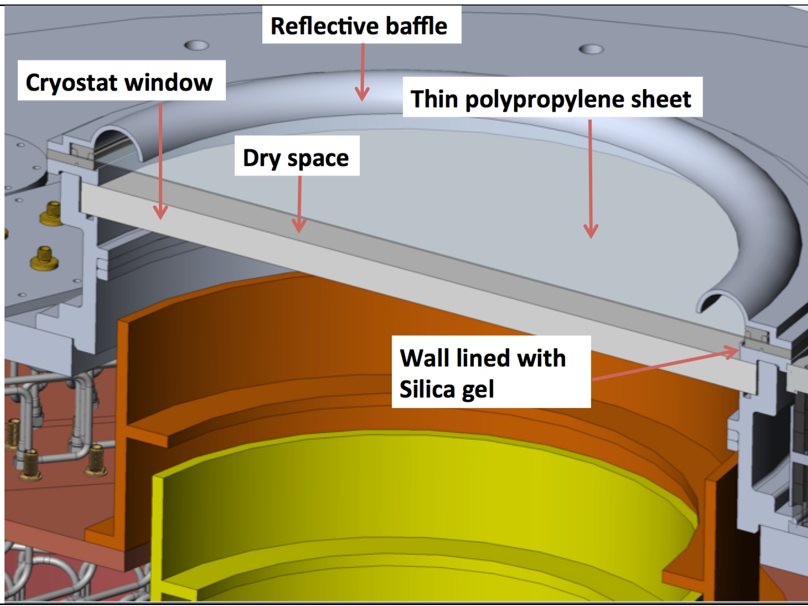

Figure 7: Window and dry space cavity

3.5 DC and RF feedthroughs

DC and RF cabling will use hermetic connectors already proven on previous instruments and test systems. These items are “off the shelf” components available from companies such as RS, Farnell and Tekdata. The intention is that no connectors will directly mate to the top plate surface but will connect via a mating flange as outlined in section 3.1. This approach allows the replacement of connectors without modification of the large cryostat top plate.

3.6 Manual heat switches

Provision is made for two manual mechanical heat switches. These are designed to connect cold (T≤ 4K) isolated stages to the high power first stage of the PTC during cool down from room temperature. We will use vacuum feedthroughs that can operate these switches that have been previously proven on test systems at Cardiff.

3.7 Arrangement of top plate

The proposed arrangement of ports and space required of the top plate is outlined in Figure 8

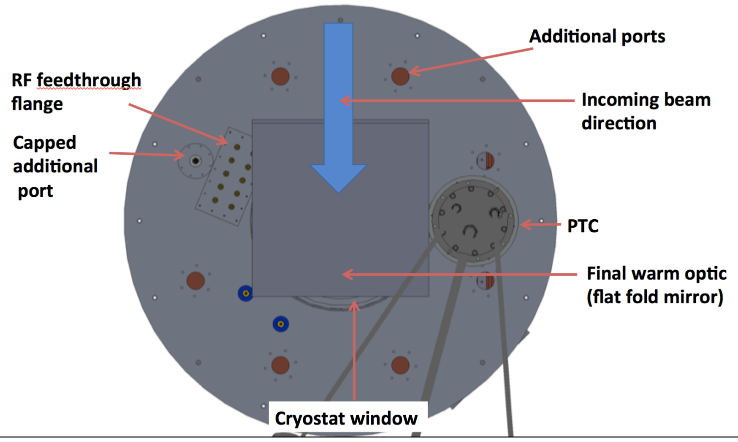

Figure 8: Top plate arrangement

3.8 Low emissivity lining

The entire vacuum vessel will be lined on the inside with magnetic shielding (detailed later in section 10) with low emissivity material on top. All surfaces not providing optical access will be lined with low emissivity material to reduce thermal load on the first stage as much as possible. The lining is held in place simply with double-sided tape a method proven on similar systems developed at Cardiff.

3.9 Vacuum vessel checklist

- The structural integrity analysis of the vessel is sufficient (assumption that this approach worked for CLOVER).
- All required ports (DC, RF, PTC and optical) have been considered and limits of adjustment are understood if small modifications are required before machining takes place.
- The Window design is fit for purpose in terms of transmission and structural integrity under vacuum (assumption that this approach worked for CLOVER and ACTpol).
- Any other issues to raise for review.

4 First Cryogenic Stage

The first cryogenic stage is 814 mm in diameter and 757mm in height (excluding optical baffle). The stage is connected to the PTC first stage via a flexible copper braid using a method previously tested at Cardiff and will sit at a temperature of around 50K (specific temperature will depend on final load). This stage is designed to:

- Provide a thermal sinking point to links between colder stages and room temperature.
- Provide radiation shielding and optical baffling to colder stages.

4.1 Mechanical support and thermal isolation

The first stage is mechanically supported by 7 stainless steel legs. We have chosen stainless steel as the support material as it offers low thermal conductivity to strength ratios and thermally contracts at the same rate as the PTC tubes. Such supports have been used in several test systems at Cardiff and have proven to be suitable. The supports for the first stage must support the mass of all cold components that have an estimated mass of 159.6kg. Each support leg for the stage consists of a 19.05mm diameter tube 75mm in length with a wall thickness of 0.56mm. A Finite Element Analysis (FEA) has been performed using SolidWorks to test the structural integrity of the entire support structure. The simulation has been run with the first stage plate in place supported by the 7 support legs. A dummy mass is added to the plate to represent the additional mass from the first stage radiation shield and colder stages (a total of 121.6 kg). The details of the simulations and its results are shown in Figure 10 and Figure 11.

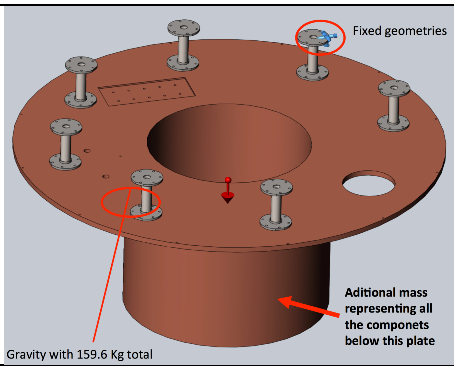

Figure 9: FEA analysis of first stage setup.

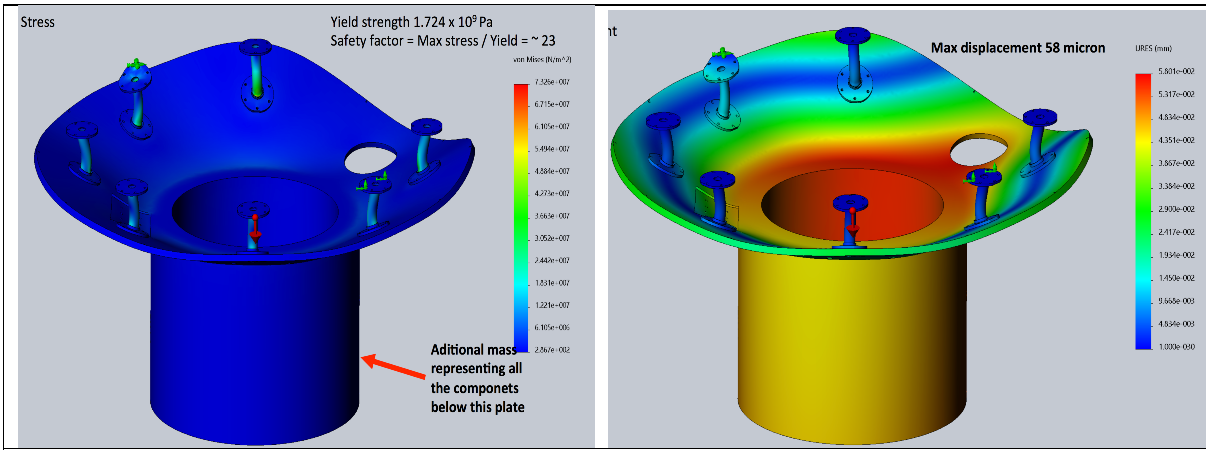

Figure 10: FEA analysis of first stage support structures (vertical).

The results shown in Figure 10 show that the support legs are sufficient to hold the mass of all cold components with a safety factor of **23** in the vertical direction. We do not anticipate any lateral forces on this system (except in transit when the support structures will be braced with travel brackets), however data from out existing systems demonstrates that these legs used in support structures are extremely strong. This is confirmed in a second simulation adding a force in the perpendicular direction as depicted in Figure 11. Here we see the maximum stress is a factor of **16** below the yield strength of the supports.

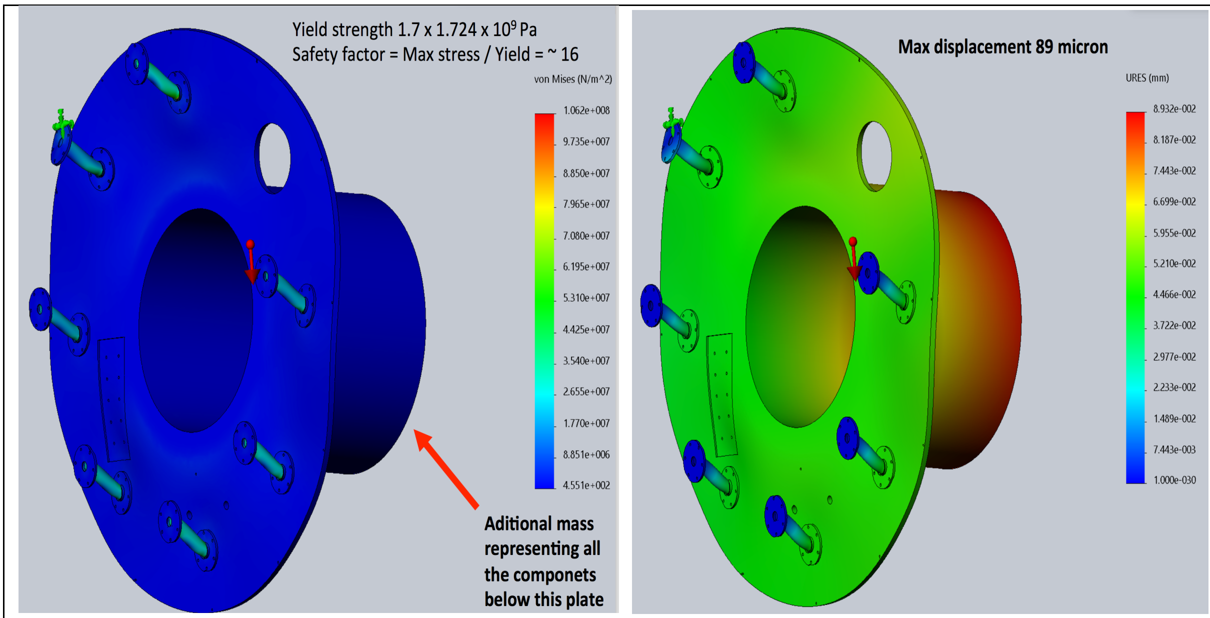

Figure 11: FEA analysis of second stage support structures (horizontal).

The thermal performance of these support structures is outlined in the cryogenics CDR document.

4.2 Thermal connections, thermal sinking and feedthroughs

The first stage plate is connected to the first stage of the PTC via a set of flexible copper braids. This approach is adopted from previous systems developed at Cardiff and the thermal details are outlined in the cryogenics CDR document. A set of fingers are formed from a plate connected to the PTC head and a second plate connected to the first stage plate. Stainless steel plates are used to form a high clamping force between the braid and copper fingers. This is depicted in Figure 12

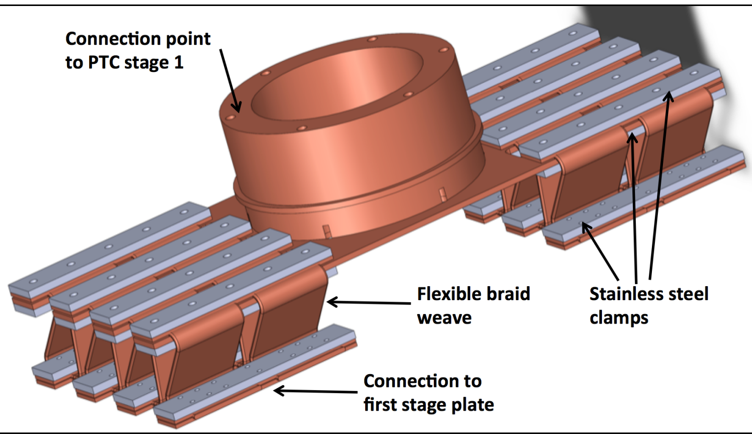

Figure 12: Copper braid assembly.

We adapt a similar approach to the vacuum plate when providing access for thermal sinking and cable feedthroughs. The second stage plate will be machined with a number of holes where custom flanges can be installed to provide feedthroughs and/or thermal sinking points for cables and other future structures. A larger dedicated space will be reserved for a series of SMA bulkhead connectors used for heat sinking RF cables and providing breakpoints for DC blocks, amplifiers and attenuators if required. An examples of the RF feedthrough point can be seen in Figure 13

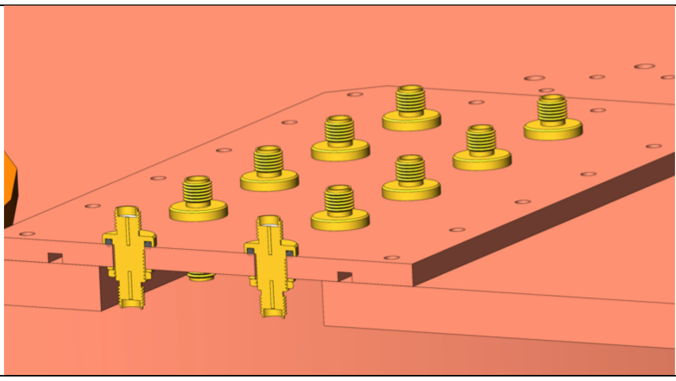

Figure 13: second stage RF feedthrough example.

4.3 Radiation shields and optical baffles

The 50K radiation shield is a simple can fabricated from rolled copper sheet soldered to a copper flange. This method has been extensively tested at Cardiff in other systems and has proven a cost effective and lightweight method of forming radiation shields. The shields are fabricated with tapped holes in the flange to bolt to the first stage plate on one side and a lid on the other. The flange is designed to be thick enough so that bolts do not protrude. The space above the flange is reserved for Multi Layer Insulation (MLI). We anticipate using around 20 layers of MLI with a thick layer of low emissivity material used for the outer most layer. The outer layer reduces the shield effective emissivity further and protects the delicate MLI when handling. This is depicted in Figure 14.

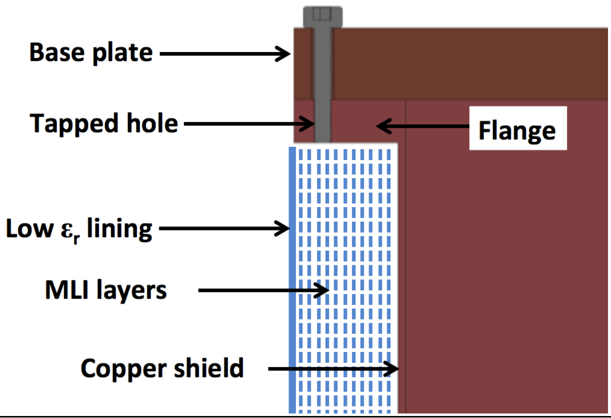

Figure 14: Radiation shield flange and MLI installation.

An optical baffle is connected to the first stage plate. This baffle shields the lower temperature stages from 300K radiation as well as providing a mounting point for optical filters. The optical filters cool primarily through radiation. The baffle provides shading from 300K radiation for the filters at this stage and provides space for thermal shading filters to reduce 300K radiation loads. Details of the baffling structures is outlined in section 9.

4.4 First stage checklist

- Is the structural support analysis and data sufficient to prove structural integrity
- All required ports and cable thermal sinking points (DC, RF and optical) have been considered and limits of adjustment are understood should small modifications be required.
- Has sufficient provision been made for MLI installation
- Any other issues to raise.

5 Second cryogenic stage

The second cryogenic stage is 726 mm in diameter and 581mm in height. The stage is connected to the PTC second stage using the same copper braid method outlined in section 4 and will sit at a temperature of around 3.5 - 4K (specific temperature will depend on final load). This stage is designed to:

- Provide a thermal sinking point to links between colder stages and the second stage.
- Provide radiation shielding, optical and optical filtering to colder stages.
- Provide a condensation point for two sets of sorption coolers used to cool sub-K stages.
- Mount the cold low noise amplifiers for the RF readout signal from the array.

5.1 Mechanical support and thermal isolation

The second stage is mechanically supported by 7 stainless steel legs chosen for the same reasons outlined in section 4. The supports for the second stage must support the mass of all cold components colder than the first stage estimated to be 92.6kg. Each support leg for the stage consists of a 15.88mm diameter tube 127mm in length with a wall thickness of 0.56mm. A Finite Element Analysis (FEA) using the same method outlined in section 4.1 is used to test the structural integrity of the entire support structure. The details of the simulations and its results are shown in Figure 15 and Figure 16.

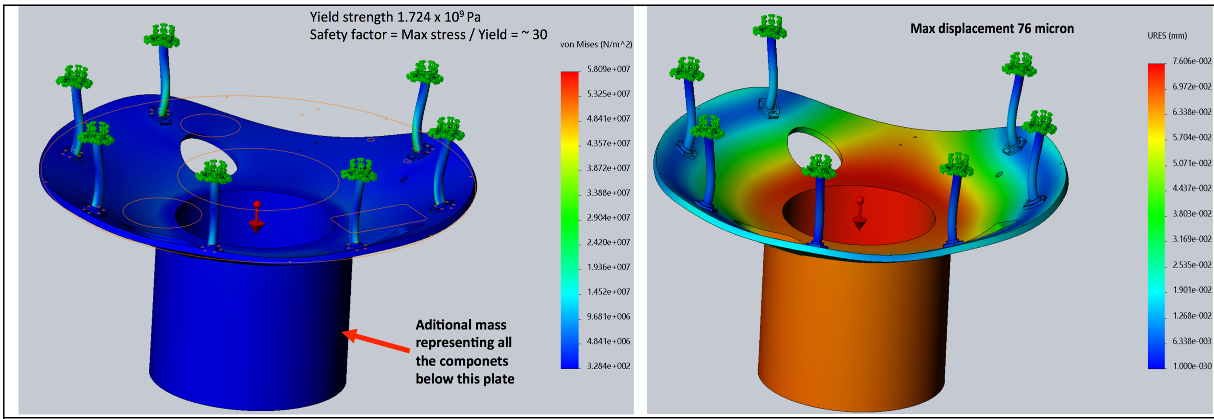

Figure 15: Second stage mechanical support FEA (vertical).

The analysis shows that the maximum stress expected is a factor of 30 below the structure yield point in the vertical direction.

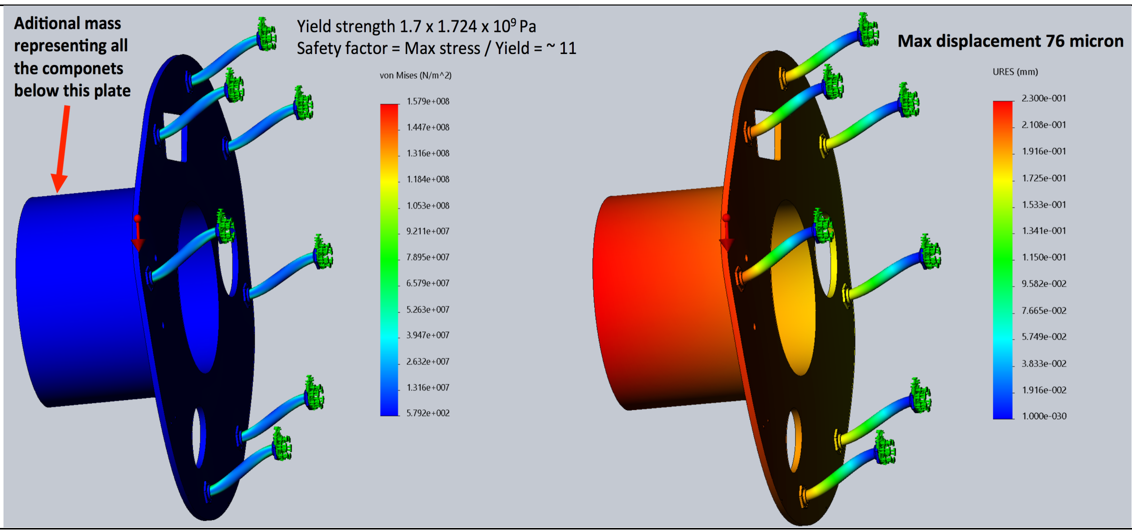

Figure 16: Second stage mechanical support FEA (horizontal).

The analysis shows that the maximum stress expected is a factor of 11 below the structure yield point in the vertical direction.

5.2 Thermal connections, thermal sinking and feedthroughs

We adopt the same approach of providing thermal connections to the PTC and provision for cable feedthrough as outlined in section 4.2 so the detail will not be repeated here.

5.3 Sorption fridge location and heat sinking

Two sorption fridge units are mounted to the second stage plate to provide continuous cooling to two sub-K stages approximately at temperatures of 1K and 350mK. These are depicted in Figure 17. Each unit uses the first stage plate to condense He4. To assist in maintaining the second stage plate at a temperature below the ^{4}He condensation point, the heat switches used to cool the sorption pumps from around 40K-5K during a cycle are connected to the PTC head directly through separate copper braids. This method avoids heating the condensation point on the first stage plate un-necessarily due to the power not having to flow through the thermal impedance set by the copper braid connecting the first stage to the PTC head.

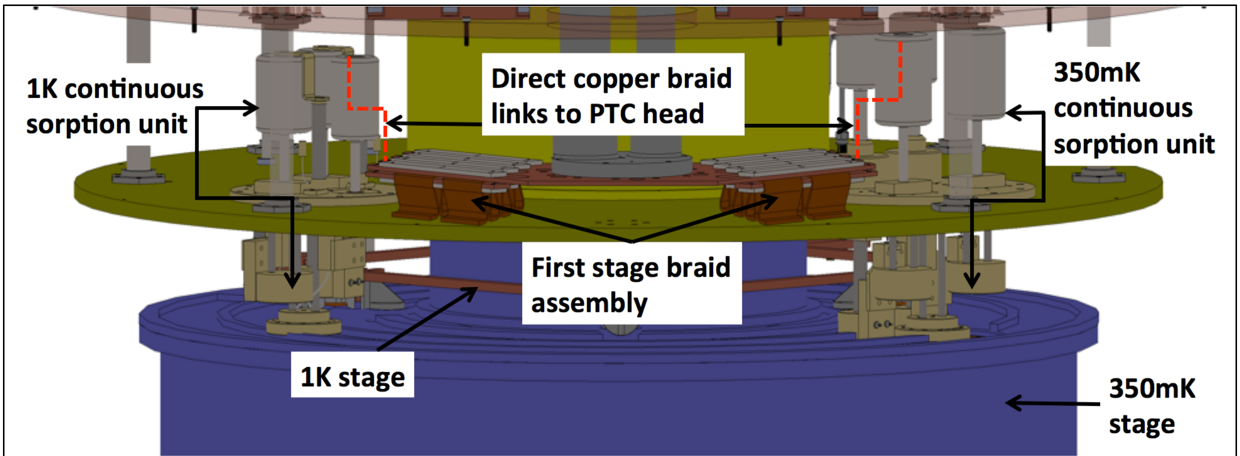

Figure 17: Sorption fridge locations

5.4 Heat switch contact point

A heat switch point is added to connect the first and second stages during initial cooling from 300K to 50K. This switch is operated by the manually turning the knob located on the cryostat top plate. The switch is depicted in Figure 18.

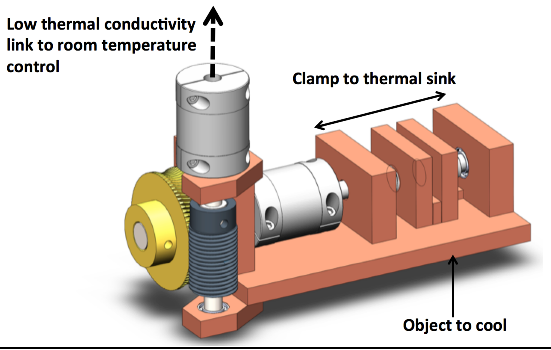

Figure 18: Mechanical heat switch.

5.5 Radiation shields and optical baffling

The radiation shields will be fabricated using a similar method outlined in section 4.3. We intend to have the option lining this stage with Cryoperm to aid magnetic shielding. This will be reviewed on a cost benefit analysis.

The shields will be lined with MLI and low emissivity lining in the same manner as outlined in section 4.3. The optical baffling and filter mounts are similar to that outlined in section 4.3 and is detailed in section 9.

5.6 Cold amplifier mounting

The cold amplifiers are mounted directly to the rigid SMA bulkhead connector mounted to a flange attached to the first stage plate. The amplifiers are heat sunk to the plate via a copper bracket as outlined in Figure 19.

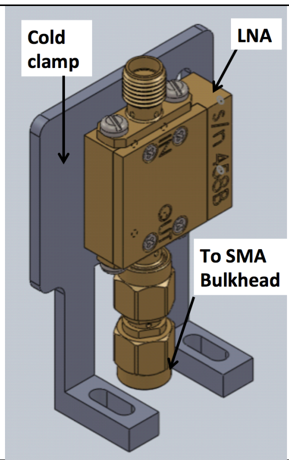

Figure 19 Example cold amplifier mounting.

5.7 Second stage checklist

- Is the structural support analysis and data sufficient to prove structural integrity
- All required ports and cable thermal sinking points (DC, RF and optical) have been considered and limits of adjustment are understood should small modifications be required.
- Has sufficient provision been made for MLI and magnetic shielding installation?
- Has space and consideration been provided for sorption fridges and dumping of power during cycling?
- Is there provision for all five cold low noise amplifiers and thermal sinking.
- Any other issues to raise.

6 First sub-K stage

The first sub-Kelvin stage consists of a Copper ring reinforced with a stainless steel ring continuously cooled by two ^{4}He sorption fridges coupled via a passive heat switch. The stage will sit at around 0.8-1.0K. This stage is designed to:

- Provide a point to heat sink mechanical supports and cables running to colder stages.

6.1 Mechanical support

The stage is supported from the second stage via four thin walled stainless steel cross structures. Provision is made both in the thermal budget and physical space to add an additional two structures if required. Running with the base line four structures has the advantage of reducing thermal loads on the stage giving cryogenic headroom and risk reduction. These structures must hold the mass at the second sub-K stage and the focal plane estimated to be of order 41.6kg. The cross structure has undergone Finite Element Analysis (FEA) in SolidWorks to test structural integrity. The results show a tendency for a single structure to twist when tested in isolation under ¼ of the expected load. This effect is shown in Figure 21. **Physical tests are currently being carried out on a single structure to test the validity of the FEA.**

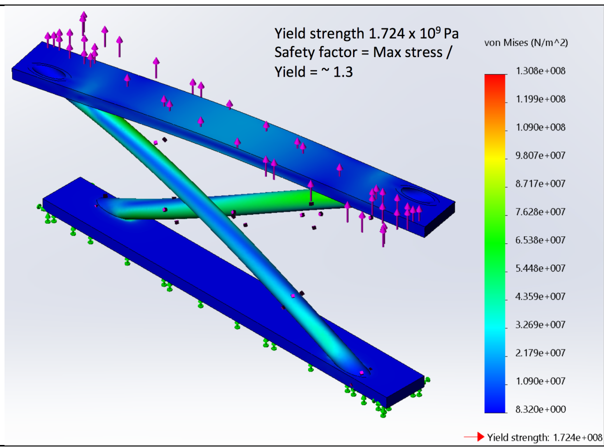

Figure 20 FEA on single support structure

When simulated as an assembly of four structures arranged in a ring configuration we find that the tendency to twist is removed and the structural strength is adequate to support the mass of the colder stages with a maximum stress **a factor of 3** below the yield point of the structure. The results of this analysis are shown in Figure 22.

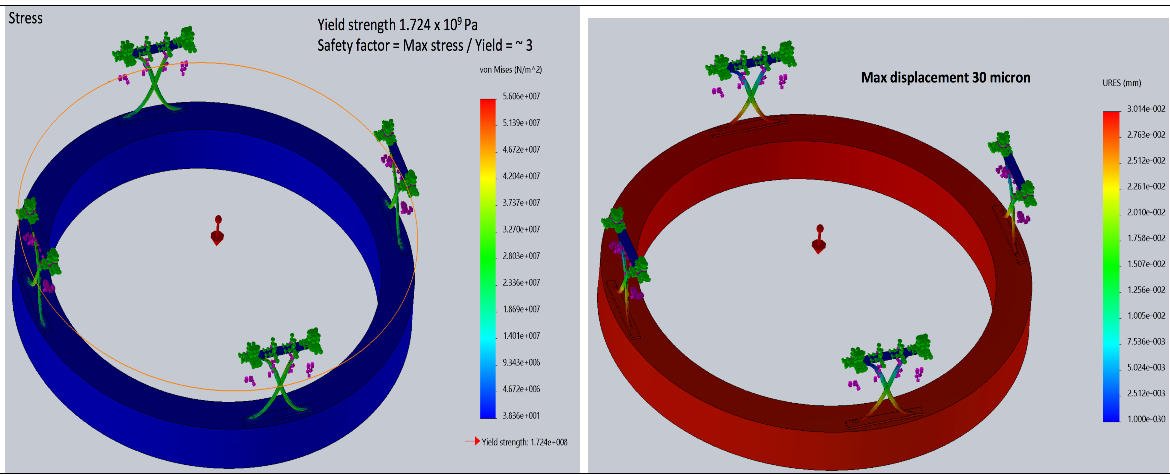

Figure 21 FEA on for support structure in a ring assembly (vertical)

The FEA analysis shows that the maximum stress in a factor of 3 below the structure yield point in the nominal vertical direction.

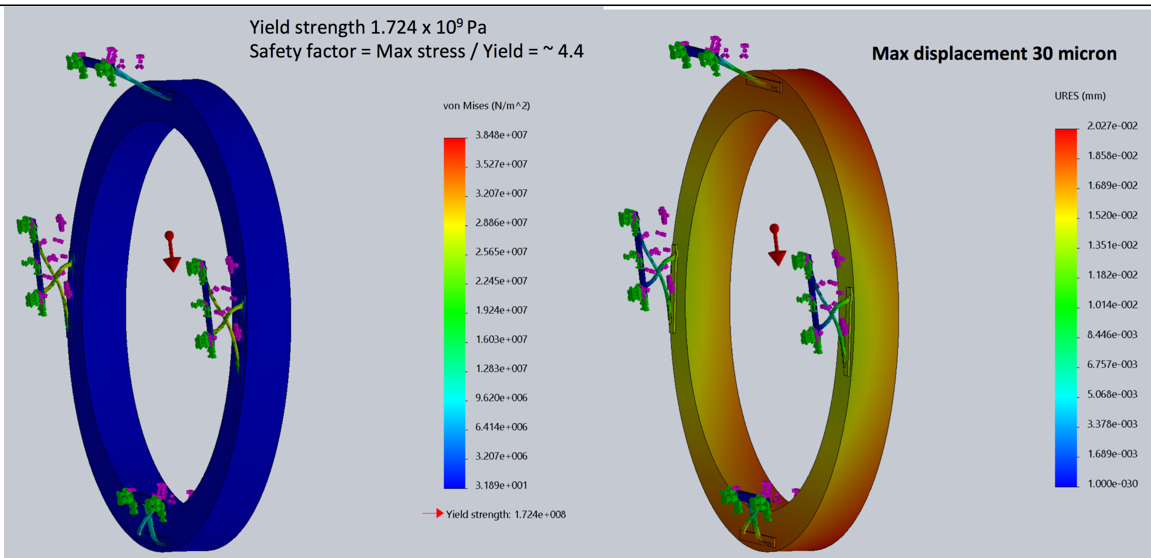

Figure 22 FEA on four support structures in a ring assembly (horizontal)

The FEA analysis shows that the maximum stress in a factor of 4.4 below the structure yield point in the nominal horizontal direction.

6.2 First sub-K stage checklist

- Is the structural support analysis and data sufficient to prove structural integrity
- All required ports and cable thermal sinking points (DC and RF) have been considered and limits of adjustment are understood should small modifications be required.
- Any other issues to raise.

7 Second sub-K stage

The second sub-K stage forms a cold box around the detectors and supports the cold optics. This stage also cools the condenser of the mini-dilutor system used to cool the focal plane. The stage is cooled to around 350mK (dependant on load) using a continuous He7 sorption unit and has a mass of 36.9kg. The stage is supported off the first sub-K stage via four sapphire joints. The purpose of this stage is to:

- Provide thermal sinking for parts running to the focal plane:
- Provide continuous 350mK platform to cool the condenser of the mini-dilutor system used to cool the focal plane
- Provide a cold box to shield the detectors and cold optics from stray radiation
- Provide a mounting point for the cold optics

7.1 Mechanical support and thermal isolation

The second sub-K stage has a diameter of 640mm and a height of 468mm. This stage is supported by four sapphire joints required to support a total mass of 39.9kg (second sub-K stage + cold optics + focal plane). Sapphire joints are a Cardiff developed technology proven on several test systems and SCUBA-2. They work by sandwiching sapphire powder between two sapphire disks creating very low contact areas between the two disks hence excellent thermal isolation. The joints are very strong but non-trivial to simulate. We therefore tested 4 joints in a test rig to measure the displacement under a 60kg load. The setup is shown in Figure 23

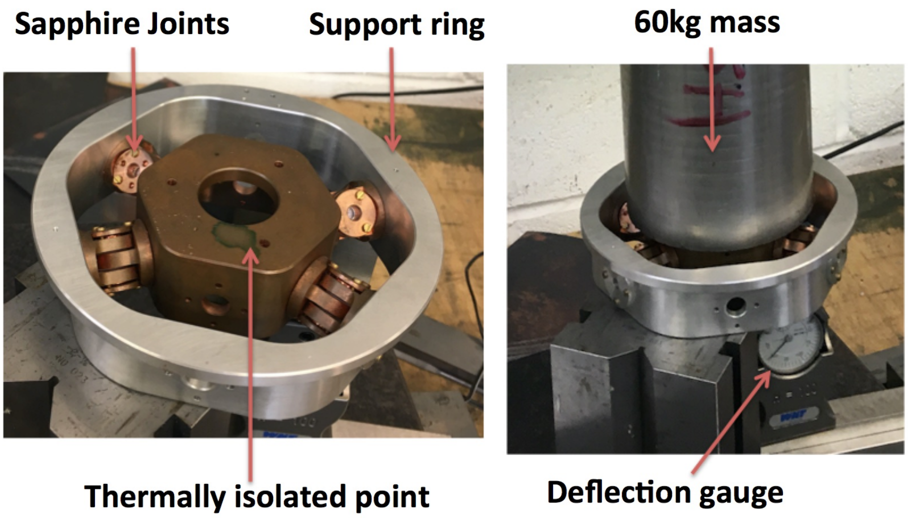

Figure 23: Sapphire joint stress test setup.

The results of these tests are outlined in Table 1.

Load /kg	Deflection /μm	Load	Deflection /μm	Load	Deflection /μm
0.0	0	0.0	5	60.6	140
20.5	20	37.9	55	0.0	50
0.0	0	0.0	10	-	-
28.1	30	32.5	60	-	-
0.0	0	0.0	15	-	-
35.9	45	40.1	70	-	-

Table 1

The results show that we see no hysteresis in the measurements up to an applied load of 28.1 kg. We begin to see modest hysteresis for loads between 35.9 and 37.9 kg and stronger hysteresis at higher loads. The hysteresis is a sign that we have moved beyond the elastic limit of the joint but at this stage it is unclear if the hysteresis is due to the joint or the supporting structure. The thermal budget for this stage is dominated by the dilutor load and adding up to four additional joints is feasible should further investigation deem it necessary.

7.2 Heat switch contact point

A heat switch as shown in Figure 18 is added to short the second sub-K stage to the first stage during cool down from 300-4K. This switch is released when the system is ready to cycle the sub-K coolers. The positions of all heat switches are depicted in Figure 24 as the system cools.

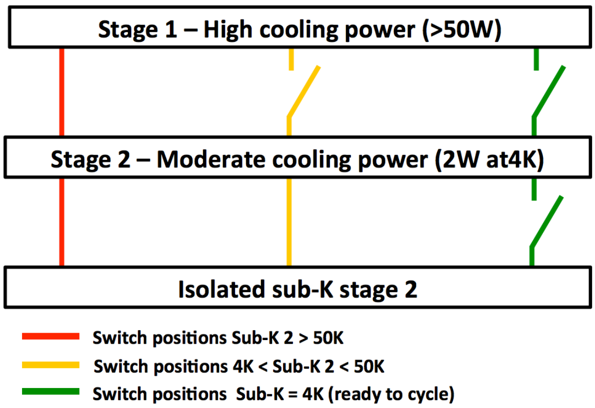

Figure 24 Second sub-K stage heat switch sequence.

7.3 Radiation and magnetic shielding

The second sub-K radiation shields and plate will form a superconducting shield around the detectors. Working at 350mK gives us three options to achieve this:

1. Create the shields from Aluminium and add an aluminium plate to the copper base. Aluminium superconducts at 1.2K.
2. Fabricate the shields as outlined in section 4.3 and coat with Niobium using a sputter coating process. This may be expensive and needs investigating. Niobium superconducts at around 9K.
3. Fabricate the shields as outlined in section 4.3 but copper weld parts together instead of soldering then coat with lead solder.

The option chosen will be investigated using a cost benefit analysis but cryogenically and mechanically all options are feasible.

7.4 Cable feedthroughs.

The same approach is adopted to providing cable feedthroughs for the second sub-K stage as outlined in section 4.2. Feedthroughs and blanking plates will be made to superconduct adopting the same method used for the radiation shield.

7.5 Dilution unit mounting point.

We are currently considering two versions of possible dilution units. For this reason detailed design on mounting of the dilution unit is incomplete. We envisage mounting the dilutor condensing point directly to the second sub-K stage plate. Additional ridged copper strapping will run directly from the continuous sorption cooler head to the dilutor condenser to ensure efficient condensation of the dilutor mash. Details of this will be outlined in the CDR meeting.

7.6 Cold optics mounting

The cold optics will be mounted directly to the second sub-K stage plate. Space has been provided based upon the current optical design and is depicted in Figure 25.

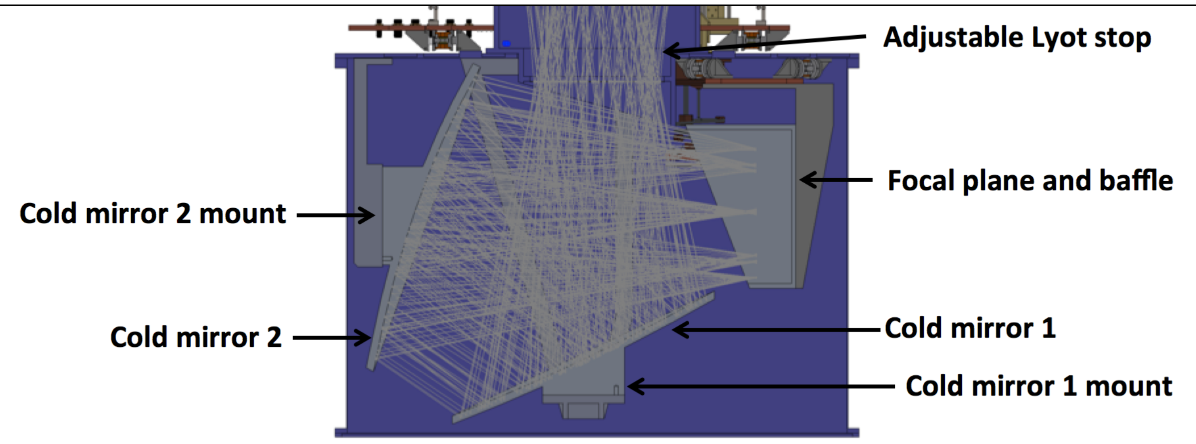

Figure 25 Cold optics and focal plane space.

7.7 Second sub-K stage checklist

- Is the structural support analysis and data sufficient to prove structural integrity with provision for additional support available if required.
- All required ports and cable thermal sinking points (DC and RF) have been considered and limits of adjustment are understood should small modifications be required.
- Provision for cold baffling and filter mounting is in place.
- Space is provided for all cold optics mounting.
- Any other issues to raise.

8 Focal plane stage

The focal plane stage is still being designed so for this review we have added a concept focal plane of the approximate dimensions required to house a 1Fλ F#3 horn coupled detector array that fills the field of view of the LMT.

8.1 Mechanical support

The focal plane will be supported from the second sub-K stage via four sapphire joints. The focal plane is expected to be less than 5kg in mass therefore given the mechanical testing presented in section 7.1 is more than sufficient to support this stage.

8.2 Cable feedthroughs, thermal links and cooling

The focal plane is not enclosed like previous stages and therefore can be directly accessed from ports located on the second sub-K plate providing that optical beam are avoided.

We will link the focal plane to the dilutor head via a solid copper link. The dilutor head is fitted with an active heat switch that can be turned on to link it to the second sub-K stage. This will be used in cooling from 300K as the second sub-K stage is connected to more powerful cooling stages as outlined in Figure 24. The active heat switch is also used when condensing the $^{4}He/^{3}He$ mash to ensure the phase boundary forms in the mixing chamber.

8.3 Focal plane checklist

- Is the structural support analysis and data sufficient to prove structural integrity.
- All required ports and cable thermal sinking points (DC and RF) have been considered and limits of adjustment are understood should small modifications be required.
- Any other issues to raise.

9 Optical baffling and filter provision

The overall design incorporates space to provide optical baffling and filtering at each stage. Internal discussion at Cardiff has come to the conclusion that filters will be provided at each stage by the way of cartages that can be mounted within each baffle tube. The cartages are expected to be 50mm in height.

9.1 Optical baffling

The stray light path illustrated in Figure 26 shows that the extremes of the array are terminated at a 4K baffle. The base line horn coupled architecture will provide additional stray light baffling.

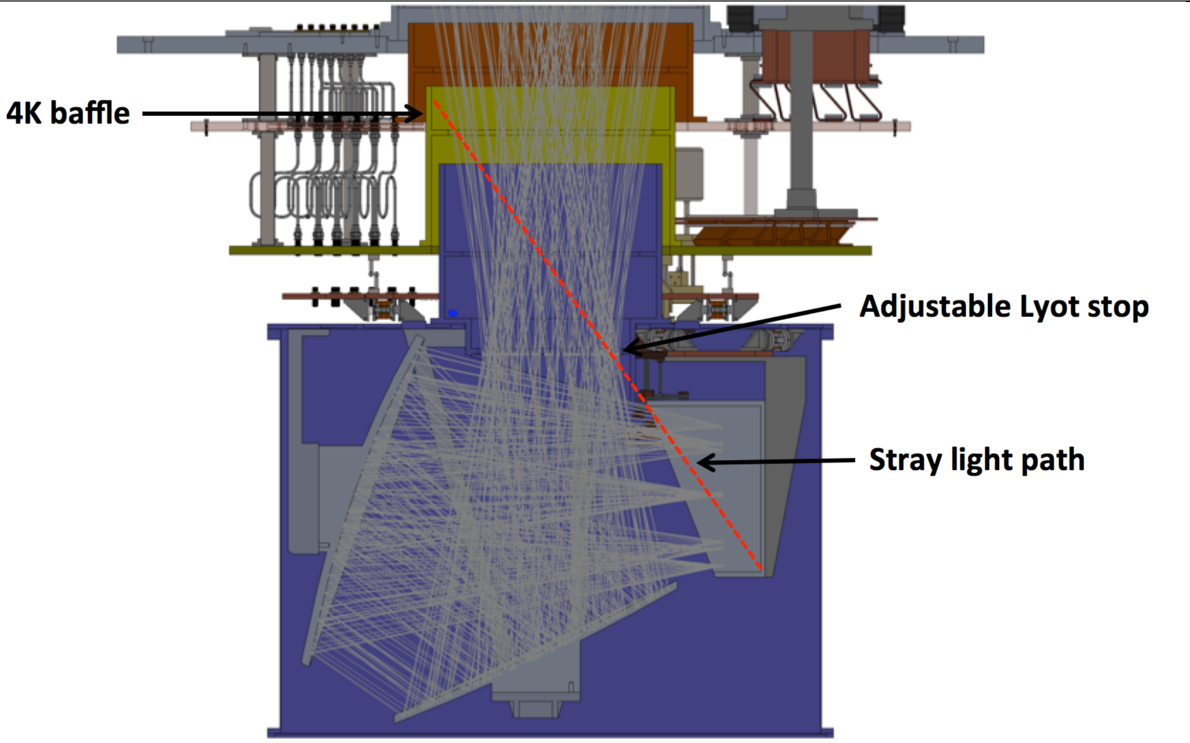

Figure 26: Stray light path and baffling.

9.2 Filter provision

Mounting points for filter cartages are provided within each baffle tube. Mounting points are located behind the window to mount thermal filters at 300K. These are secured using a circlip and reduce the effective window emissivity to around 10%. Space is provided for mounting a Lyot stop that can vary in size and tilt angle to suit a range of optical solutions. The filter and Lyot stop mounts are depicted in Figure 27.

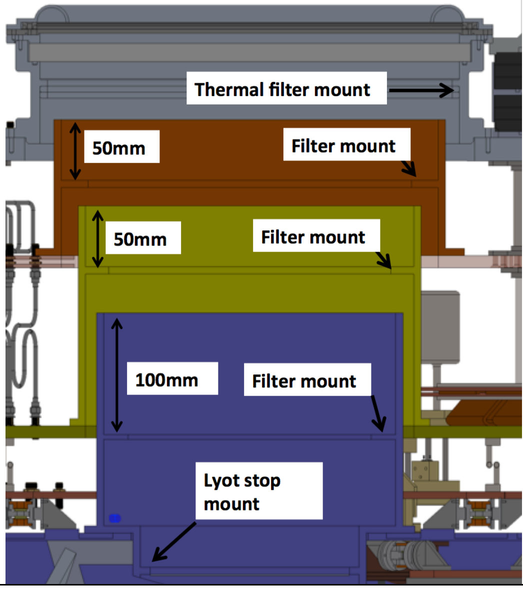

Figure 27: Filter mounting.

10 Magnetic shielding provision

Magnetic shielding is not well defined for KID arrays and many eefects can be mitigated by geometry considerations of the KID architecture. We have adopted the approach of a base line option of:

- Room temperature Finemet or Cryoperm shielding at 300K
- A superconducting shield on the second (350mK) stage

We will make provision for an additional Cryoperm shielding at 4K. Magnetic sielding will be discussed in more detail at the CDR meeting.

11 Assembly

We have solutions in place for assembly and access to arrays and filters after the system build is complete. The detail is difficult to document so these will be discussed in detail at the CDR meeting with the aid of a slide set.

12 Apendix

12.1 Mass breakdown

Mass details at each stage are outlined in Table 2

Stage	Detector	Sub-K 2	Sub-K 1	Second	First	Vacuum
T/K (approx)	0.1	0.35	1.0	3.5	50	300
Plate /kg	0.5	7 .0	1.7	29.4	38.0	33
Can / kg	0.5	10.5	-	16.1	22.0	64
Lid /kg	2.0	3.0	-	4.3	5.5	30
Baffle /kg	-	3.7	-	1.1	1.0	
Optics + Dilutor	-	12.7	-	-	-	-
PTC + misc						48.3
Total	3.0	36.9	1.7	51.0	67.0	175.3
Accumulated	3.0	39.9	41.6	92.6	159.6	334.9

Table 2